# A Novel Porous Bone Scaffold Made with 3D Bioprinter Using Carboxymethyl Chitosan-Hyaluronic Acid for Knee Repair: Mechanical and Chemical Properties

***Jasemi, Amir; Zibaseresht, Ramin*+; Jalali Monfared, Marzieh***
*Biomaterials and Medicine Chemistry Research Centre, Aja University of Medical Sciences, Tehran, I.R. IRAN*

***Ehsan, Nassireslami; Zahra, Hami***
*Toxicology Research Center, AJA University of Medical Sciences, Tehran; I.R. IRAN*

***Fatah Hesari, Shamim***
*Orthopedic Surgeon, Department of Surgery, Imam Reza Hospital, Tehran, I.R. IRAN*

***Fasihi, Hossein***
*Biomaterials and Medicine Chemistry Research Centre, Aja University of Medical Sciences, Tehran, I.R. IRAN*

**Abstract:** *Porous bone scaffolds are made by various methods such as membrane lamination, space holder, freeze-drying, and 3D printing techniques. With the advent of 3D printing, this method has emerged as a new tool for designing porous scaffolds. The porous scaffolds are expected to have a multifunctional effect and changing porosity patterns as an approach to integrating the mechanical properties of different designs into a unique scaffold design. The knees, as a large joint, in addition to helping the limbs, also bear the weight of the body. In this study, the bone scaffold was fabricated using materials such as carboxymethyl chitosan (CCHI) and hyaluronic acid (HLA) using a three-dimensional bioprinter method for repairing the knee joint bone. In this study, Scanning Electron Microscopy (SEM) analysis is used to study morphology. In order to investigate the existing phases, phase changes due to different content to determine the absence of space particles in the production scaffold and to determine the size of blocks by X-Ray Diffraction (XRD). The MTT toxicity, apatite formation, as well as cell growth tests, were used to evaluate the biocompatibility and biodegradability of the porous scaffold. The scaffold degradation rate is determined after immersion in Simulated Body Fluid (SBF) as well as Phosphate Buffer Saline (PBS). The outcome shows that the sample with 10 wt% HLA presents suitable mechanical and biological properties compared to the pure sample.*

**KEYWORDS:** *Bone Scaffold; Knee Repair; 3D Printer; Tissue engineering; Hyaluronic acid.*

*****To whom correspondence should be addressed.*
**+** *E-mail: rzi12@uclive.ac.nz*
*1021-9986/2023/7/2141-2152* *12/$/6.02*

## INTRODUCTION

Today, in medical science and tissue engineering, biocompatible and absorbable polymeric materials are used to repair and regenerate bone and cartilage tissue [1-3]. The main and most important function of bone is to provide a hard and strong framework for the human body, which in addition to protecting soft organs such as the brain, heart, and lungs, allows the person to move with the help of muscles [4-7]. However, the bone function is not limited to these components. In addition to providing the ability to move and provide mechanical protection to vulnerable organs, bone also plays a vital role in the hematopoietic process. In addition, there is a close connection between this tissue and the immune system. Because the source of type B lymphocytes, which are responsible for producing the right antibodies for the body's defenses can be the bone marrow [8-12]. Bone also acts as a source of calcium storage for the bone and body. The presence of calcium ions is essential for muscle contraction, blood coagulation, permeability of cell membranes, transmission of nerve pulses, etc. [13-17]. Bone stores about 99% of the total calcium in the body and the human body receives a significant amount of calcium for its daily needs from this source [14-19]. In addition, calcium ions can control and balance minerals in the body fluids [18-25]. The calcium performance and all these tasks and functions are responsible for bone. Bones are one of the dynamic microstructures that can heal after a fracture or injury. However, the severity of the injury should be considered [26-36]. The bone with compact and spongy architecture can be treated by artificial bone substitutes. Porous bone has lower compressive strength than dense bone, however, it is more resistant to impact force. Recently, the fabrication of porous bone, implants have been considered because of its similarity to bone tissue and the higher similarity of the bone implant with the bone structure leads to more suitable healing of the damaged tissue [37-42].

Although bones are self-healing organs in the human body, they have weak properties in many diseases such as osteoporosis, bone marrow cancer, sarcoma, or severe injuries caused by accidents. Porous scaffolds have good mechanical properties in addition to bioactivity [43-52]. Porous bone scaffold is a new method of cancer treatment, especially bone replacement for hyperthermia treatment and bone fracture by orthopedic surgeons. Tissue engineering, known as the design and construction of new tissue to evaluate the function of defective organs or lost tissue. The principles of tissue engineering are cellular, molecular biological expansion, and tissue formation based on biological properties. The cells' function and the structure of the extracellular matrix (ECM) create a suitable environment for cell adhesion and maintenance as a key concept [62-67].

Bone tissue engineering necessarily requires three components such as bone progenitor cells, bone Growth Factors (GFs), and scaffold for adhesion and maintenance of cell function [68-71]. The most important advantage of tissue engineering is that connective tissue can be produced outside the body which cannot harm the living body. Stem cells have a high potential for cell therapy and tissue engineering due to their self-renewal properties and ability to differentiate into different cells including osteoblasts affected by host tissue or culture medium. One of the methods of making absorbable polymer implants is a 3D printer, which provides the possibility of printing natural polymers in bone tissue engineering. The 3D printers have been able to play the role of the link between the science of tissue engineering materials. Therefore, various methods have been developed to produce tissue engineering scaffolds by 3D printing using computer systems.

## EXPERIMENTAL SECTION

In this study, a porous scaffold made of 3D printing methods with good accuracy and structure with the desired texture. Also, the speed of preparation of porous scaffold is very high and economical. The 3D printing methods usually have two main stages such as the production of a computer design for the desired organ and the second stage is the implementation of this design by 3D printers for bone substitutes. To prepare the novel bio-nanocomposite, 30 grams of carboxymethyl chitosan (CCHI) and 10 cc of glutaraldehyde were added to the standard glass tube. Then, to create cross-links for the bio-nanocomposite, the polymers were dissolved in the 68 cc polymers and mixed for 4 hours on the magnetic stirrer. After that two 2 Bio-Oss Tablet drugs weighing 2 grams were mixed into the solution and kept on the magnetic stirrer.The samples were prepared by 0, 5, and 10 wt% of hyaluronic acid (HLA) added to the solution. After preparing the bio nanocomposite, the samples were prepared by 3D Bioprinter of

*Table 1: A list of raw materials for the preparation of porous scaffold*

| Materials | Amount | Abbreviation |
|---|---|---|
| Carboxymethyl chitosan | 30 g | CCHI |
| Hyaluronic Acid | 30 g | HLA |
| Glutaraldehyde | 10 cc | - |
| Distilled water | 1 L | - |
| Bio-Ossteointegradation | 10 g | Bio-Oss |

OMIDAFARINAN company X Fab3 with the cubic geometry designed by solid work. The aim of this research was to fabricate and evaluate a 3D porous scaffold using a 3D bioprinter machine for the repair of knee joints using Bio-Oss bone supplement. The prepared samples were examined for compressive strength tests, porosity measurement, bioactivity, and biodegradability evaluations. The materials characterization such as scanning Electron Microscope (SEM), X-Ray Diffraction (XRD), and Fourier-Transform InfraRed (FT-IR) Spectroscopy techniques at Biomaterials and Medicine Chemistry Research Centre, Aja University of Medical Sciences. The biocompatible properties of the porous scaffold and apatite formation for biological investigation are considered in this study. The sample preparation was done according to the starting materials according to Table 1. The XRD analysis was done by the Philips X' part at a distance of 0 to 90° and in the range 2θ. The X' pert High score plus software was also used to determine the size of the crystals. Using this test, we can check the amount of agglomeration and determine the particle size. To perform the SEM analysis, the LEO-435VP device was used at an applied voltage of 30 kW. The bioactivity evaluation and their rate of apatite formation as well as the evaluation of pH of scaffolds with 0, 5, and 10% of hyaluronic acid was considered in the Simulated Body Fluid (SBF) which is a very similar composition to human body blood developed by *Kokubo et al* [79]. This solution has a concentration similar to human blood plasma, which is maintained under temperature and physiological pH of the body. Phosphate Buffer Saline (PBS) is a water-based saline solution consisting of sodium chloride, sodium phosphate, and in some formulation potassium chloride and potassium phosphate. In this test, 5 PBS tablets are dissolved in 90 mL of deionized water and after complete dissolution of the tablets, the volume of the solution is increased to 1000 mL. The PBS in this solution helps to keep the pH of the solution constant, and also because it is both concentrated with the body's biological substances and the solution is non-toxic, it has many uses for the human body [80]. The solution should be stored in a sterile space under the hood using a 0.22-micron filter at 4℃. The mechanical strength was performed to evaluate the tensile strength and bearing capacity of the porous scaffold according to ASTM standards. The mechanical performance of the porous scaffold was done in order to control the quality and predict how a substance may react under other types of forces. The stress-strain curve is plotted based on the amount of applied force elongation, so the test output is a stress/strain curve that indicates the behavior of the material under tension.

The tendency of a fluid to spread on the surface of a solid in the presence of other miscible salts is called wettability. By measuring the angle of contact of the solid with the liquid, this tendency to spread on the solid surface can be measured. This contact angle is between the numbers 0 and 180°, with an angle of 0 representing a more complete and an angle of 180° representing an absolute non-absolute. As the angle decreases, the properties of the fluid increase. This test shows the wetting of scaffolds made with different weight percentages of hyaluronic acid.

## RESULTS AND DISCUSSION

### *XRD analysis*

To investigate the phase of prepared sample and the pure materials, it is shown that the presence of amorphous materials in porous CCHI-HLA scaffold with 0, 5 and 10 wt% of HLA has amorphous architecture as shown in Fig. 1. The XRD pattern shows that the sample with higher amount of HLA has a lower sharp peak.

Fig. 1 shows that only large peaks, characteristic of amorphous structures for the three samples. Also, it shows the presence of high crystallinity in the final membranes which can be ruled out. Also, the FT-IR was performed using FTIR-JASCO680 PLUS device.

### *SEM analysis*

The SEM analysis was used to evaluate the amount and size of porosity as well as the morphology of porous CCHI-HLA porous scaffolds containing 0, 5, and 10 wt% of HLA. The amount of porosity on the surface of the sample, the size of the cavities, the relationship of the porosity, and the porosity shape can be seen by SEM analysis.

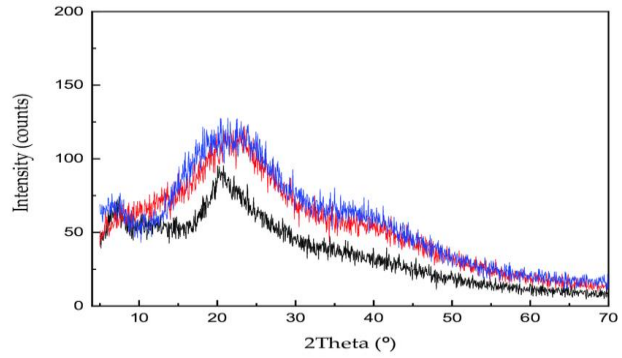


***Fig. 1: XRD pattern of the optimal sample for bone scaffold with CCHI and various amounts of HLA***

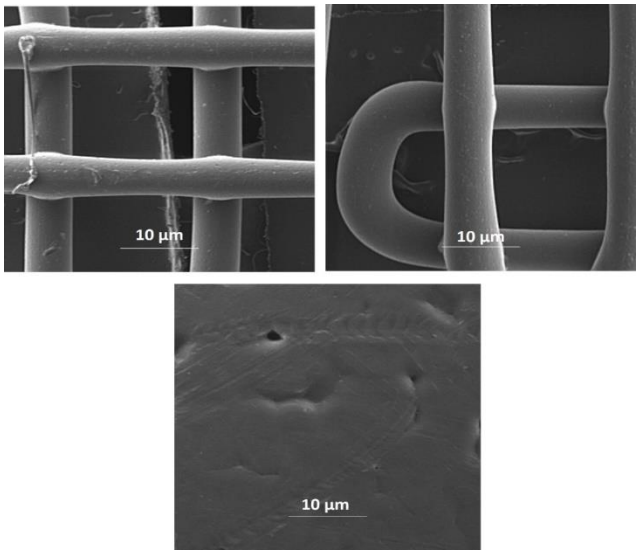


***Fig. 2: SEM image of porous bone scaffold with CCHI-HLA***

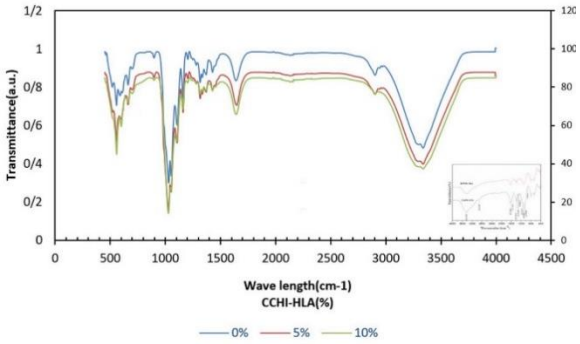


***Fig. 3: FTIR analysis CCHI-HLA in the range of 250 to 4000 $cm^{-1}$***

Fig. 2 shows a SEM image of a three-dimensional (3D) bioprinted scaffold made of CCHI-HLA. As the size of the hole and pores in the scaffold are too large, the cells can easily moved into the dark space and to their desired direction without getting stuck at the fiber-binding vertices. Also, the initial cell proliferation and mechanical properties of the prepared bony scaffold can be impaired. In contrast, as the size of the porosity is small size, it becomes more difficult for nutrients to reach the cells and excrete the waste products from them. It should be noted that the percentage of porosity and pore size are very important for scaffolds made of two components. The minimum porosity and cavity size for bone tissue growth are 65-70% and 100-200 µm, respectively. As the porosity size and shape are closed, the porosity does not reach the scaffold surface. The open porosity with one or more paths can help the cells to reach the surface and improve the ossification process with an appropriate porosity as shown in Fig. 2.

### *FTIR analysis*

In order to examine the CCHI-HLA scaffold containing various amounts of HLA which is soaked in SBF solution can confirm excellent the cross-linking of the based matrix and additive in the range of 250 to 4000 $cm^{-1}$. The FT-IR results indicated that the preparation of porous scaffold using glutaraldehyde has been successfully performed and can be used for transverse connections.

### *Porosity evaluation of porous scaffold*

Porosity is the main and influential factor on the mechanical properties and structural integrity of scaffold. Among the important and prominent features in the design and construction of scaffold the shape, size, volume, roughness, and distribution of cavities is important. In fact, the size of the pores and their internal 3D relationship are very important for better cell expansion and angiogenesis. In this study, the Image-J software was used to investigate the porosity percentage of porous CCHI-HLA scaffolds containing 0, 5, and 10 wt% of HLA. For this purpose, with the support of SEM images and Image-J software, the percentage of porosity of porous scaffolds with different amounts of HLA was investigated and presented in Fig. 4. Fig. 4 shows that with the addition of HLA to the CCHI the porosity percentages increase using 3D bioprinter technique using the following Eq. (1).

$$\text{Porosity}\ (\%) = (W1 - W3)/(W2 - W3) \times 100 \qquad (1)$$

Several studies have shown in tissue engineering applications for the preparation of orthopedic bony scaffolds, open porosity is suitable for nutrient transport and target tissue formation [55-67]. On the other hand, due to the similarity

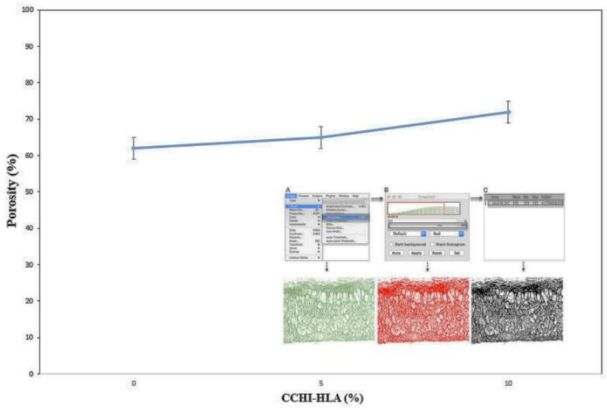


*Fig. 4: Porosity evaluation of bone scaffold with CCHI-HLA using SEM images and Image-J software*

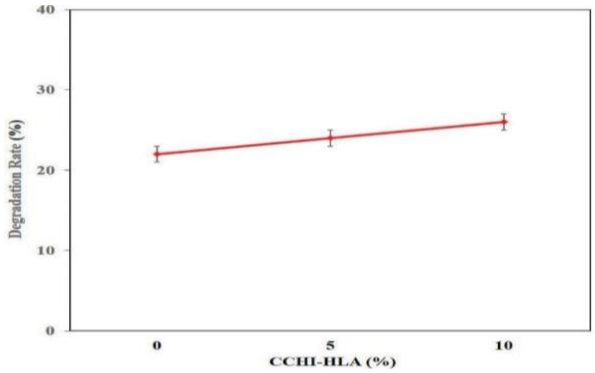


*Fig. 6: Comparison of the degradation rate of the bone scaffold with CCHI-HLA in PBS*

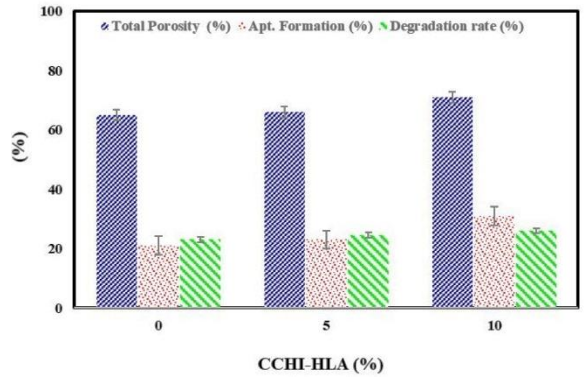


*Fig. 7: Results of comparison of porosity compared to the results of apatite formation and degradation rate*

of the regular scaffold with the natural tissue structure in the body, the fibers became clumped, reduced in diameter, and distributed. In contrast, the tensile strength increased from 1.2 MPa to 4.1 MPa. The agglomeration of the two polymers changes the porosity value of the scaffold. Therefore, the elastic modulus and tensile strength of the sample with the highest percentage of HLA can reach the maximum amount which can be a good choice to replace the sponge bone. As shown in Fig. 4, the porosity of the scaffold increases from 65% to 71% and the growth rate of apatite increases from 20% to 31%. However, the dissolution result shows that the sample has become a rubbery form. Also, the results indicated that the addition of HLA did not significantly increase or decrease in weight of the sample in the biological investigation in a PBS or SBF environment.

***Apatite formation and degradation rate of porous scaffolds***

The apatite formation in the SBF to evaluate the rate of apatite formation was done. In this test, by consuming the calcium and phosphate ions present in the SBF, the apatite formation begins to grow spontaneously on the porous 3D surface. During this test, after placing the scaffold in the Falcon tube pouring the SBF on it, and placing it in the water bath at 37°C after 1, 4, 7, 14, and 21 days, the apatite formation mechanism and pH changes were determined. Also, the degradation rate of porous scaffolds has been investigated and presented in Fig. 5 and Fig. 6.

A careful review of the relevant articles shows that most of the samples made in the biomaterial field for bone replacement remain only as theoretical species, while in this study, a significant achievement was achieved the dissolution rate of the samples is very low as shown in Fig. 6. Surface roughness is an important factor affecting the reaction between cells and tissue engineering scaffolds and changing cellular behavior. The nanometric roughness of the hyaluronic acid scaffold, due to its similarity to the body's natural ECM, increases the absorption of proteins such as fibronectin and vitronectin and increases cell proliferation and viability

As can be seen in the porous scaffold consisting of carboxymethyl chitosan, and glutaraldehyde with different percentages of 0, 5, and 10 wt% of hyaluronic acid, increasing the amount of HLA in the scaffold has been associated with an increase in porosity and apatite formation. Although the amount of degradability increased in samples consisting of 0 wt% and 5 wt% HLA.

The wettability test is to check the degree of CCHI-HLA porous scaffold with 0, 5, and 10 wt% of hyaluronic acid. By increasing the amount of hyaluronic acid, the wetting contact angle increased from 124.8 to 125.7 and then decreased to 113.9 as shown in Fig. 8. The decrease in wetting indicates the increase in the hydrophilicity of in the samples, and the increase in hyaluronic acid has

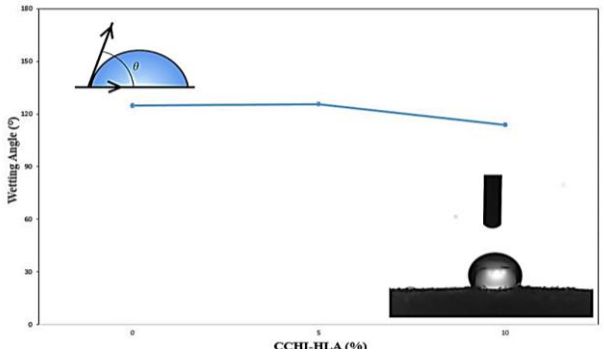


*Fig. 8: Results of Wettability test of the bone scaffold with CCHI-HLA containing various amounts of HLA*

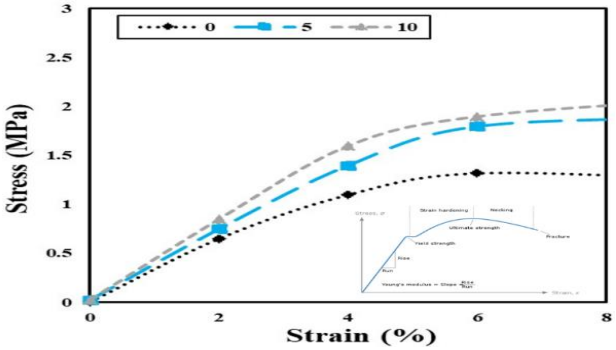


*Fig. 9: Results of stress-strain diagram of bone scaffold with carboxymethyl chitosan- Hyaluronic acid base material*

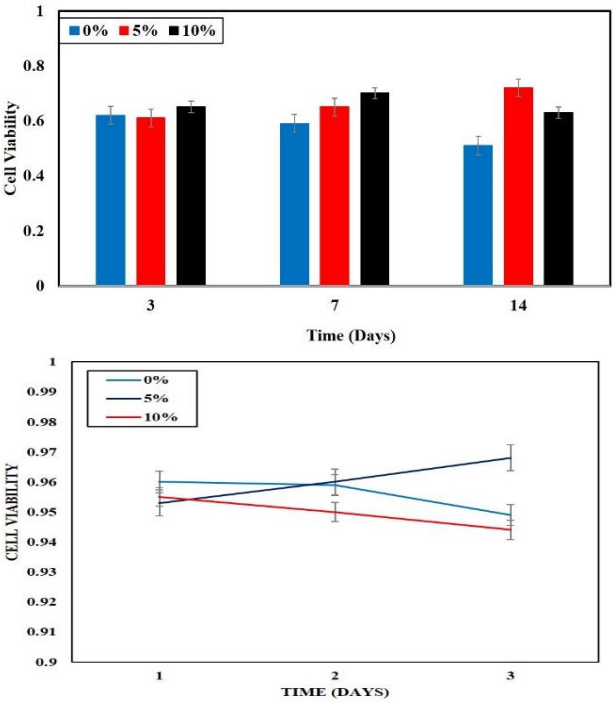


*Fig. 10: Results of Cell viability of bone scaffold with carboxymethyl chitosan- Hyaluronic acid base material*

increased the hydrophilicity of the scaffolds. This hydrophilicity of the scaffolds shows the water absorption of the scaffolds and also the non-accumulation of water in the knee joint preventing the knee from getting infected.

In this paper, various micromechanical methods are proposed to obtain the effective elastic properties of bone scaffolds. The investigation of the mechanical properties of various scaffolds shows proper modeling of single-scale ceramic scaffolds and modeling of composite polymer material scaffolds in the fabrication of bone scaffolds. As can be seen, with the increase in the amount of hyaluronic acid in the scaffolds, the amount of tension also increases, which increases the amount of strain in the scaffolds and the elastic modulus can also be obtained by calculating the slope of the stress-strain as shown in Fig. 9.

In order to prepare the culture medium, 10 g of DMEM powder containing L-Glutamine along with 3.7 g of sodium bicarbonate powder was poured into an Erlenmeyer containing 900 mL of deionized water plus 100 micrograms of streptomycin and 100 units of Penicillin per mL. The pH of the prepared solution was adjusted to 7.2 using one molar Hydrochloric Acid (HCL). Then, the solution was brought to a volume of 1000 mL and kept under the hood by a 0.22 micro-style filter in sterile glass containers at 4°C. The flask culture vessel is flushed after being coated with adherent cells, and the cells are washed with PBS solution and trypsin enzyme is added to the flask and incubated at 37°C for 3 to 5 minutes. Among all the methods used to determine cell proliferation, MTT test is the most preferred assay. This test is evaluated using the STAT FAX 2100 Microplate Reader, ELISA Analyzer with 545 nm wavelength based on the amount of color change in which wells with more cells have a higher Optical Density (OD) than wells with fewer cells. This test was performed in the Pasteur Institute of Iran for 1, 3 and 7 days as shown in Fig. 10.

Fig. 10 shows the amount of cell growth in 1, 3, and 7 days. In this period of time, the sample containing 5 wt% hyaluronic acid, compared to the sample without the presence of hyaluronic acid faced a continuous increase and increased from 0.61 to 0.72. However, in the sample with 10 wt% of hyaluronic acid, the cell growth first increased by 0.7, but then it decreased. The amount of cell growth is shown linearly, which shows the increasing trend of the sample with 5 wt% hyaluronic acid compared to the other two samples. In fact, the decrease in cell growth in the sample with 10 wt% can be due to the decrease in pH

following the increase in hyaluronic acid. Also, it is due to the presence of an acidic environment and the higher percentage of degradation of the sample.

Determining the surface roughness depends on the type of cell, scaffold, and tissue that can be achieved by changing the parameters of the electrospinning device to the optimal value. Therefore, the bone growth rate is high, bone formation is easier and the patient recovers quickly. The use of this scaffold as the main nucleus of bone growth for patients whose spinal cord, jaw and any part of their body bones are damaged. Researchers examined chitosan containing nanoparticles of Bioactive Glass (BG) and hydroxyapatite (HA) found that increasing the concentration of nanoparticles reduced the decomposition temperature and degradation occurred at lower temperatures with the addition of 1.5 wt% BG. *Khandan et al*. [24] added apatite particles to the bredigite nanoceramics. Many studies have shown that the mechanical properties and cellular behaviors in the 25% apatite sample were higher than the 50% sample Surface wettability is an important physical property in electrified scaffolds that directly affects cellular activity. *Khandan et al*. [24-25] conducted a study that showed that the water contact angle in polymeric-hydroxyapatite sample decreased compared to PCL and the hydrophilicity of the composite fibers increased due to the high wettability of the calcium phosphate phase. After examining the samples made with the support of three-dimensional bioprinters and examining the structure and morphological behavior of scaffolds made containing CCHI and HLA for use in bone tissue that are damaged due to fractures and aging, the third sample can be considered as an optimal sample. Due to the process of long-term self-healing or non-reconstruction in severe injuries, tissue engineering has been raised. The most important success factors in tissue engineering are the use of appropriate cells and scaffolds. For this purpose, various cells such as ossifiers and embryonic and mesenchymal stem cells were used in this study and the application of Bio-Oss was considered which will be presented in another article. However, the unique properties of mesenchymal cells (MSCs) have led to their widespread application in the field of tissue engineering. There are various techniques such as 3D bioprinter, freeze-drying and electrospinning for scaffold preparation [65-78]. The electrospinning method has been considered due to the similarity of nanofibers with ECM of natural tissue, the ability to choose different materials, the ratio of surface to large volume of fibers, and the regeneration of tissue as much as possible compared to other methods [74-78]. Carboxymethyl chitosan is known as a synthetic biopolymer that is widely used in medical applications for bone tissue regeneration.

## CONCLUSIONS

The choice of porous scaffold for orthopedic application using an appropriate fabrication method and cell type are key factors in the success of tissue engineering. Polymers, ceramics, and polymer-ceramic composites have been used in the manufacture of novel porous scaffolds recently. The desired membrane should be biocompatible, biodegradable, and strong and not irritate the host tissue. In this study, it was found that in order to improve hydrophilic properties, mechanical strength, proliferation and cell growth of CCHI, natural ceramics and HLA can be added to CCHI. However, the use of high concentrations of the polymer causes particles to clump and reduce the biological properties of the porous bony scaffold. On the other hand, high water absorption promotes cell interaction with fibers. In general, porous bio-nanocomposite scaffolds had better and more suitable properties than pure samples. Evaluations are ongoing to improve the properties of the scaffold and bring it closer to the body. The porosity of scaffold increases from 65% to 71% and the growth rate of apatite increases from 20% to 31% with a growth of 10%. However, the dissolution result shows that the sample has become rubbery and has not shown a significant increase or decrease in weight soaked in the PBS solution. Due to the increase in the amount of hyaluronic acid, the amount of hydration decreases. By increasing the amount of hyaluronic acid, the wetting contact angle increased from 124.8° to 125.7° and then decreased to 113.9°. The decrease in wetting indicates the increase in the hydrophilicity of the samples, and the increase in hyaluronic acid has increased the hydrophilicity of the porous scaffolds. The rate of cell growth in the time periods of 1, 3, and 7 days showed an increase of 18% in the sample with 5 wt% of hyaluronic acid.

**Acknowledgments**

We acknowledge the Toxicology Research Center, Biomaterials and Medicine Chemistry Research Centre, Aja University of Medical Sciences, Toxicology Research Center, AJA University of Medical Sciences and also Orthopedic Surgeon, Department of Surgery, Imam Reza hospital, Tehran, Iran for their kind support.

*Received : Sep. 24 , 2022 ; Accepted : Dec. 05 , 2022*

**REFERENCES**


[1] Seyedi S.Y., Salehi F., Payandemehr B., Hossein S., Hosseini-Zare M.S., Nassireslami E., Yazdi B.B Sharifzadeh M., Dual Effect of cAMP Agonist on Ameliorative Function of PKA Inhibitor in Morphine-Dependent Mice, *Fundamental & Clinical Pharmacology*, **28(4)**: 445–454 (2014).

[2] Nassireslami E., Nikbin P., Amini E., Payandemehr B., Shaerzadeh F., Khodagholi F., Yazdi B.B., Kebriaeezadeh A., Taghizadeh G., Sharifzadeh M., How Sodium Arsenite Improve Amyloid β-Induced Memory Deficit?, *Physiology & Behavior* **163**: 97–106 (2016).

[3] Amini E., Nassires**la**mi E., Payandemehr B., Khodagholi F., Foolad F., Khalaj S., Hamedani M.P., Azimi L., Sharifzadeh M., Paradoxical Role of PKA Inhibitor on Amyloidβ-Induced Memory Deficit, *Physiology & Behavior*, **149**: 76–85 (2015).

[4] Nassireslami E., Nikbin P., Payandemehr B., Amini E., Mohammadi M., Vakilzadeh G., Ghadiri T., Noorbakhsh F., Sharifzadeh M., A cAMP Analog Reverses Contextual and Tone Memory Deficits Induced by a PKA Inhibitor in Pavlovian Fear Conditioning, *Pharmacology, Biochemistry, and Behavior*, **105**: 177–182 (2013).

[5] Zarei M., Pourahmad J., Nassireslami E., Toxicity of Arsenic on Isolated Human Lymphocytes: The Key role of Cytokines and Intracellular Calcium Enhancement in Arsenic-Induced Cell Death, *Main Group Metal Chemistry*, **42(1):** 125-134 (2019).

[6] Asadi M.S., Mirghazanfari S.M., Dadpay M., Nassireslami E., Evaluation of Wound Healing Activities of Pomegranate (Punica Granatum-Lythraceae) Peel and Pulp, *JRMDS*, **6(3):** 230-236 (2018).

[7] Zarei M., Pourahmad J., Aghvami M., Soodi M., Nassireslami E., Lead Acetate Toxicity on Human Lymphocytes at Non-Cytotoxic Concentrations Detected in Human Blood, *Main Group Metal Chemistry*, **40(5-6)**: 105-112.

[8] Afshary K., Chamanara M., Talari B., Rezaei P., Nassireslami E., Therapeutic Effects of Minocycline Pretreatment in the Locomotor and Sensory Complications of Spinal Cord Injury in an Animal Model, *Journal of Molecular Neuroscience: MN*, **70(7)**: 1064–1072 (2020).

[9] Hajmirzaeyian, A., Chamanara, M., Rashidian, A., Shakyba, S., Nassireslami, E., Akhavan-Sigari, R. Melatonin Attenuated the Behavioral Despair Induced by Acute Neurogenic Stress through Blockade of N-Methyl D-Aspartate Receptors in Mice, *Heliyon*, **7(1)**: e05900 (2021).

[10] Elahabaadi E., Salarian A.A., Nassireslami E., Design, Synthesis, and Molecular Docking of Novel Hybrids of Coumarin-Dithiocarbamate Alpha-Glucosidase Inhibitors Targeting Type 2 Diabetes Mellitus. *Polycyclic Aromatic Compound*, 1–11 (2021).

[11] Sahranavard M., Akhavan Rezayat, A., Zamiri Bidary M., Omranzadeh A., Rohani F., Hamidi Farahani R., Hazrati E., Mousavi S.H., Afshar Ardalan M., Soleiman-Meigooni S., Hosseini-Shokouh S.J., Hejripour Z., Nassireslami E., Laripour R., Salarian A., Nourmohammadi A., Mosaed R., Cardiac Complications in COVID-19: A Systematic Review and Meta-Analysis, *Archives of Iranian Medicine*, **24(2)**: 152–163 (2021).

[12] Daud S.M.S.M., Yusof M.Y.P.M., Heo C.C., Khoo L.S., Singh M.K.C., Mahmood M.S., Nawawi H., Applications of Drone in Disaster Management: A Scoping Review, *Science & Justice*, **62(1)**: 30-42 (2022).

[13] Yusof N.A.M., Noor E., Reduwan N.H., Yusof M.Y. P.M., Diagnostic Accuracy of Periapical Radiograph, Cone Beam Computed Tomography, and Intrasurgical Linear Measurement Techniques for Assessing Furcation Defects: A Longitudinal Randomised Controlled Trial, *Clinical Oral Investigations*, **25(3)**: 923-932 (2021).

[14] Yusof N.A.M., Noor N., Yusof M.Y.P.M., The Accuracy of Linear Measurements in Cone Beam Computed Tomography for Assessing Intrabony and Furcation Defects: A Systematic Review and Meta-Analysis, *Journal of Oral Research*, **8(6)**: 527-539 (2019).

[15] Yusof M.Y.P.M., Mah M.C., Reduwan N.H., Kretapirom K., Affendi N.H.K., Quantitative and Qualitative Assessments of Intraosseous Neurovascular Canals in Dentate and Posteriorly Edentulous Individuals in Lateral Maxillary Sinus Wall, *The Saudi Dental Journal*, **32(8)**: 396-402 (2020).

[16] Mohammad N., Yusof M.Y.P.M., Ahmad R., Uad A. M., Region-Based Segmentation and Classification of Mandibular First Molar Tooth Based on Demirjian's Method, *I. Journal of Physics: Conference Series*, **1502(1):** 012046 (2020).

[17] Khandan A., Abdellahi M., Ozada N., Ghayour H., Study of the Bioactivity, Wettability and Hardness Behaviour of the Bovine Hydroxyapatite-Diopside Bio-Nanocomposite Coating. Journal of the Taiwan Institute of Chemical Engineers, **60**: 538-546 (2016).

[18] Ismail A.F., Othman A., Mustafa N. S., Kashmoola M.A., Mustafa B.E., Yusof M.Y.P.M., Accuracy of Different Dental Age Assessment Methods to Determine Chronological Age Among Malay Children, *Journal of Physics: Conference Series*, **1028(1):** 012102 IOP Publishing, (2018).

[19] Yusof M.Y.P.M., Rahman N.L.A., Asri A.A.A., Othman N.I., Mokhtar I.W., Repeat Analysis of Intraoral Digital Imaging Performed by Undergraduate Students Using a Complementary Metal Oxide Semiconductor Sensor: An Institutional Case Study, *Imaging science in dentistry*, **47(4)**: 233-239 (2017).

[20] Angelakopoulos N., Galić I., Balla S.B., Kiş H.C., Gómez Jiménez L., Zolotenkova G., ... Cameriere R., Comparison of the Third Molar Maturity Index (I3M) Between Left and Right Lower Third Molars to Assess the Age of Majority: A Multi-Ethnic Study Sample, *International Journal of Legal Medicine*, **135(6)**: 2423-2436 (2021).

[21] Adam F.A., Mohd N., Rani H., Baharin B., Yusof M.Y.P.M., Salvadora Persica L. Chewing Stick and Standard Toothbrush as Anti-Plaque and Anti-Gingivitis Tool: A Systematic Review and Meta-Analysis, *Journal of Ethnopharmacology*, **274**: 113882 (2021).

[22] Mohammad N., Muad A.M., Ahmad R., Yusof M.Y. P.M., Reclassification of Demirjian's Mandibular Premolars Staging for Age Estimation Based on Semi-Automated Segmentation of Deep Convolutional Neural Network, *Forensic Imaging*, **24**: 200440 (2021).

[23] Kazemi A., Abdellahi M., Khajeh-Sharafabadi A., Khandan A., Ozada N., Study of in Vitro Bioactivity and Mechanical Properties of Diopside Nano-Bioceramic Synthesized by a Facile Method Using Eggshell as Raw Material, *Materials Science and Engineering*: *C*, **71**: 604-610 (2017).

[24] Khandan A., Ozada N., Bredigite-Magnetite (Ca7MgSi4O16-Fe3O4) Nanoparticles: A Study on their Magnetic Properties, *Journal of Alloys and Compounds*, **726**: 729-736 (2017).

[25] Khandan A., Jazayeri H., Fahmy M.D., Razavi, M., Hydrogels: Types, Structure, Properties, and Applications, *Bioma.t Tiss. Eng.*, **4(27)**: 143-69 (2017).

[26] Sharafabadi A.K., Abdellahi M., Kazemi A., Khandan A., Ozada N., A Novel and Economical Route for Synthesizing Akermanite (Ca2MgSi2O7) Nano-Bioceramic, *Materials Science and Engineering: C*, **71**: 1072-1078 (2017).

[27] Shayan A., Abdellahi M., Shahmohammadian F., Jabbarzare S., Khandan A., Ghayour H., Mechanochemically Aided Sintering Process for the Synthesis of Barium Ferrite: Effect of Aluminum Substitution on Microstructure, Magnetic Properties and Microwave absorption, *Journal of Alloys and Compounds*, **708**: 538-546 (2017).

[28] Heydary H. A., Karamian E., Poorazizi E., Khandan A., Heydaripour J. A Novel Nano-Fiber of Iranian Gum Tragacanth-Polyvinyl Alcohol/Nanoclay Composite for Wound Healing Applications, *Procedia Materials Science*, **11**:176-182 (2015).

[29] Karamian E., Khandan A., Kalantar Motamedi M.R., Mirmohammadi H., Surface Characteristics and Bioactivity of a Novel Natural HA/Zircon Nanocomposite Coated on Dental Implants, *BioMed Research International*, (2014).

[30] Jabbarzare S., Abdellahi M., Ghayour H., Arpanahi A., Khandan A., A Study on the Synthesis and Magnetic Properties of the Cerium Ferrite Ceramic, *Journal of Alloys and Compounds*, **694**: 800-807 (2017).

[31] Razavi M., Khandan A., Safety, Regulatory Issues, Long-Term Biotoxicity, and the Processing Environment. Nanobiomaterials Science, Development and Evaluation, *Woodhead Publishing*, 261-279 (2017).

[32] Khandan A., Ozada N., Karamian E., Novel Microstructure Mechanical Activated Nano Composites for Tissue Engineering Applications. *J/ Bioeng/ Biomed/ Sci*., **5(1)**: 1 (2015).

[33] Ravi G.R., Subramanyam R.V., Calcium Hydroxide-Induced Resorption of Deciduous Teeth: A Possible Explanation, *Dental Hypotheses*, **3(3)**: 90. (2012).

[34] Anttonen V., Tanner T., Kämppi A., Päkkilä J., Tjäderhane L., Patinen P., A Methodological Pilot Study on Oral Health of Young, Healthy Males, *Dental Hypotheses*, **3(3)**: 106 (2012).

[35] Gupta R., Thakur N., Thakur S., Gupta B., Gupta M., Talon Cusp: A Case Report with Management Guidelines for Practicing Dentists, *Dental Hypotheses*, **4(2)**:67 (2013).

[36] Kjaer I., External Root Resorption: Different Etiologies Explained from the Composition of the Human Root-Close Periodontal Membrane, *Dental Hypotheses*, **4(3)**: 75 (2013).

[37] Motamedi M.R.K., Behzadi A., Khodadad N., Zadeh A.K., Nilchian F., Oral Health and Quality of Life in Children: a Cross-Sectional Study, *Dental Hypotheses*, **5(2)**: 53 (2014).

[38] Narayanan N., Thangavelu L. Salvia Officinalis in Dentistry. Dental Hypotheses, **6(1)**: 27 (2015).

[39] Khandan A., Karamian E., Bonakdarchian M., Mechanochemical Synthesis Evaluation of Nanocrystalline Bone-Derived Bioceramic Powder Using for Bone Tissue Engineering, *Dental Hypotheses*, **5(4)**: 155 (2014).

[40] Mosallaeipour S., Nejad M.G., Shavarani S.M., Nazerian R., Mobile Robot Scheduling for Cycle Time Optimization in Flow-Shop Cells, A Case Study, *Production Engineering*, **12(1)**: 83-94 (2018).

[41] Ghasemi M., Nejad, M.G., Bagzibagli K., Knowledge Management Orientation: An Innovative Perspective to Hospital Management, *Iranian Journal of Public Health*, **46(12)**: 1639 (2017).

[42] Ghadiri Nejad M., Husseinzadeh Kashan A., Shavarani S.M., A Novel Competitive Hybrid Approach Based on Grouping Evolution Strategy Algorithm for Solving U-shaped Assembly Line Balancing Problems, *Production Engineering*, **12(5)**: 555-566 (2018).

[43] Karamian E., Motamedi M.R.K., Khandan A., Soltani P., Maghsoudi S., An in Vitro Evaluation of Novel NHA/Zircon Plasma Coating on 316L Stainless Steel Dental Implant, *Progress in Natural Science: Materials International*, **24(2)**: 150-156 (2014).

[44] Karamian E., Abdellahi M., Khandan A., Abdellah S., Introducing the Fluorine Doped Natural Hydroxyapatite-Titania Nanobiocomposite Ceramic, *Journal of Alloys and Compounds*, **679**: 375-383 (2016).

[45] Najafinezhad A., Abdellahi M., Ghayour H., Soheily A., Chami A., Khandan A., A Comparative Study on the Synthesis Mechanism, Bioactivity and Mechanical Properties of Three Silicate Bioceramics, *Materials Science and Engineering: C*, **72**: 259-267 (2017).

[46] Ghayour H., Abdellahi M., Ozada N., Jabbrzare S., Khandan A., Hyperthermia Application of Zinc Doped Nickel Ferrite Nanoparticles, *Journal of Physics and Chemistry of Solids*, **111**: 464-472 (2017).

[47] Saeedi M.R., Morovvati M.R., Mollaei-Dariani B., Experimental and Numerical Investigation of Impact Resistance of Aluminum–Copper Cladded Sheets Using an Energy-Based Damage Model, *Journal of the Brazilian Society of Mechanical Sciences and Engineering*, **42(6)**: 1-24 (2020).

[48] Kardan-Halvaei M., Morovvati M.R., Mollaei-Dariani B., Crystal Plasticity Finite Element Simulation and Experimental Investigation of the Micro-Upsetting Process of OFHC Copper, *Journal of Micromechanics and Microengineering*, **30(7)**: 075005 (2020).

[49] Fazlollahi M., Morovvati M.R., Mollaei Dariani B., Theoretical, Numerical and Experimental Investigation of Hydro-Mechanical Deep Drawing of Steel/Polymer/Steel Sandwich Sheets, *Proceedings of the Institution of Mechanical Engineers, Part B: Journal of Engineering Manufacture*, **233(5)**: 1529-1546 (2019).

[50] Saeedi M.R., Morovvati M.R., Alizadeh-Vaghasloo Y., Experimental and Numerical Study of Mode-I and Mixed-Mode Fracture of Ductile U-Notched Functionally Graded Materials, *International Journal of Mechanical Sciences*, **144**: 324-340 (2018).

[51] Morovvati M.R., Mollaei-Dariani B., The Formability Investigation of CNT-Reinforced Aluminum Nano-Composite Sheets Manufactured by accumulative Roll Bonding, *The International Journal of Advanced Manufacturing Technology*, **95(9)**: 3523-3533 (2018).

[52] Morovvati M.R., Dariani B.M., The Effect of Annealing on the Formability of Aluminum 1200 After Accumulative Roll Bonding, *Journal of Manufacturing Processes*, **30:** 241-254 (2017).

[53] Morovvati M.R., Lalehpour A., Esmaeilzare A., Effect of Nano/Micro B4C and SiC Particles on Fracture Properties of Aluminum 7075 Particulate Composites under Chevron-Notch Plane Strain Fracture Toughness Test, *Materials Research Express*, **3(12)**: 125026 (2016).

[54] Fatemi A., Morovvati M.R., Biglari F.R., The Effect of Tube Material, Microstructure, and Heat Treatment on Process Responses of Tube Hydroforming Without Axial Force, The *International Journal of Advanced Manufacturing Technology*, **68(1)**: 263-276 (2013).

[55] Pourmoghadam M.N., Esfahani R.S., Morovvati M., R., Rizi B.N., Bifurcation Analysis of Plastic Wrinkling Formation for Anisotropic Laminated Sheets (AA2024–Polyamide–AA2024), *Computational Materials Science*, **77**: 35-43 (2013).

[56] Morovvati M.R., Fatemi A., Sadighi M., Experimental and Finite Element Investigation on Wrinkling of Circular Single Layer and Two-Layer Sheet Metals in Deep Drawing Process, *The International Journal of Advanced Manufacturing Technology*, **54(1)**: 113-121 (2011).

[57] Morovvati M.R., Mollaei-Dariani B., Haddadzadeh M., Initial Blank Optimization in Multilayer Deep Drawing Process Using GONNS, *Journal of Manufacturing Science and Engineering*, **132(6)**: (2010).

[58] Fatemi A., Biglari F., Morovvati M.R., Influences of Inner Pressure and Tube Thickness on Process Responses of Hydroforming Copper Tubes Without Axial Force., Proceedings of the Institution of Mechanical Engineers, Part B: *Journal of Engineering Manufacture*, **224(12)**: 1866-1878 (2010).

[59] Anarestani S.S., Morovvati M.R., Vaghasloo Y.A., Influence of Anisotropy and Lubrication on Wrinkling of Circular Plates Using Bifurcation Theory, *International Journal of Material Forming*, **8(3)**: 439-454 (2015).

[60] Monfared, R.M., Ayatollahi, M.R., Isfahani, R.B., Synergistic Effects of Hybrid WCNT/Nanosilica on the Tensile and Tribological Properties of Woven Carbon Fabric Epoxy Composites, *Theoretical and Applied Fracture Mechanics*, **96**: 272-284 (2018).

[61] Kamarian S., Bodaghi M., Isfahani R.B., Song J.I. Thermal Buckling Analysis of Sandwich Plates with Soft Core and CNT-Reinforced Composite Face Sheets, *Journal of Sandwich Structures & Materials*, **23(8)**: 3606-3644 (2021).

[61] Kamarian S., Bodaghi M., Isfahani R. B., Song, J. I., A Comparison Between the Effects of Shape Memory Alloys and Carbon Nanotubes on the Thermal Buckling of Laminated Composite Beams, *Mechanics Based Design of Structures and Machines*, **50(7)**: 2250-2273 (2022).

[62] Barbaz-I R., "Experimental Determining of the Elastic Modulus and Strength of Composites Reinforced with Two Nanoparticles", Doctoral Dissertation, MSc Thesis, School of Mechanical Engineering Iran University of Science and Technology, Tehran, Iran (2014).

[63] Monfared R.M., Ayatollahi M.R., Isfahani R.B., Synergistic Effects of Hybrid MWCNT/Nanosilica on the Tensile and Tribological Properties of Woven Carbon Fabric Epoxy Composites. Theoretical and Applied Fracture Mechanics, **96**: 272-284 (2018).

[64] Kamarian S., Bodaghi M., Isfahani R.B., Song J.I., Thermal Buckling Analysis of Sandwich Plates with Soft Core and CNT-Reinforced Composite Face Sheets, *Journal of Sandwich Structures & Materials*, **23(8)**: 3606-3644 (2021).

[65] Kamarian S., Bodaghi M., Isfahani R.B., Song, J.I., A Comparison Between the Effects of Shape Memory Alloys and Carbon Nanotubes on the Thermal Buckling of Laminated Composite Beams, *Mechanics Based Design of Structures and Machines*, **50(7)**: 2250-2273 (2022).

[66] Barbaz-I, R. Experimental Determining of the Elastic Modulus and Strength of Composites Reinforced with Two Nanoparticles (Doctoral Dissertation, Doctoral Dissertation, PhD Thesis, School of Mechanical Engineering Iran University of Science and Technology, Tehran, Iran), (2014).

[67] Mahjoory M., Shahgholi M., Karimipour A., The Effects of Initial Temperature and Pressure on the Mechanical Properties of Reinforced Calcium Phosphate Cement with Magnesium Nanoparticles: A Molecular Dynamics Approach. International Communications in Heat and Mass Transfer, **135**: 106067 (2022).

[68] Talebi M., Abbasi-Rad S., Malekzadeh M., Shahgholi M., Ardakani A.A., Foudeh K., Rad H.S., Cortical Bone Mechanical Assessment *via* free Water Relaxometry at 3 T, *Journal of Magnetic Resonance Imaging*, **54(6)**: 1744-1751 (2021).

[69] Shahgholi M., Oliviero S., Baino F., Vitale-Brovarone C., Gastaldi D., Vena P., Mechanical Characterization of Glass-Ceramic Scaffolds at Multiple Characteristic Lengths through Nanoindentation, *Journal of the European Ceramic Society*, **36(9)**: 2403-2409 (2016).

[70] Fada R., Farhadi Babadi N., Azimi R., Karimian M., Shahgholi M., Mechanical Properties Improvement and Bone Regeneration of Calcium Phosphate Bone Cement, Polymethyl Methacrylate and Glass Ionomer, *Journal of Nanoanalysis*, **8(1)**: 60-79 (2021).

[71] Shahgholi M., Firouzi P., Malekahmadi O., Vakili S., Karimipour A., Ghashang M., Hussain W., , Kareem H.A., Baghaei S., Fabrication and Characterization of Nanocrystalline Hydroxyapatite Reinforced with Silica-Magnetite Nanoparticles with Proper Thermal Conductivity, *Materials Chemistry and Physics*, (2022).

[72] Lucchini R., Carnelli D., Gastaldi D., Shahgholi M., Contro R., Vena P., A Damage Model to Simulate Nanoindentation Tests of Lamellar Bone at Multiple Penetration Depth, in: ECCOMAS 2012 - European Congress on Computational Methods in Applied Sciences and Engineering, E-Book Full Papers, 5919–5924 (2012).

[73] Jafari H., Danaee I., Eskandari H., RashvandAvei M., Electrochemical and Theoretical Studies of Adsorption and Corrosion Inhibition of N, N′-bis (2-Hydroxyethoxyacetophenone)-2, 2-Dimethyl-1, 2-Propanediimine on Low Carbon Steel (API 5L Grade B) in Acidic Solution, *Industrial & Engineering Chemistry Research*, **52(20)**: 6617-6632 (2013).

[74] Jafari H., Danaee I., Eskandari H., RashvandAvei M., Combined Computational and Experimental Study on the Adsorption and Inhibition Effects of $N_2O_2$ Schiff Base on the Corrosion of API 5L Grade B Steel in 1 mol/L HCl, *Journal of Materials Science & Technology*, **30(3)**: 239-252 (2014).

[75] Jafari H., Ameri E., Soltanolkottabi F., Berisha A., Seydou M., Experimental and Theoretical Investigations of New Schiff Base Compound Adsorption on Aluminium in 1 M HCl, *Journal of Electrochemical Science and Engineering* (2022).

[76] Samadian S., Karbalaei A., Pourmadadi M., Yazdian F., Rashedi H., Omidi M., Malmir S., A Novel Alginate-Gelatin Microcapsule to Enhance Bone Differentiation of Mesenchymal Stem Cells, *International Journal of Polymeric Materials and Polymeric Biomaterials*, **71(6)**: 395-402. (2022).

[77] Shahmoradi S., Yazdian F., Janghorbani A., Satarian L., Behroozi F., Tabandeh F., Navaei-Nigjeh M., Applying Differentiated Retinal Cell for Age-related Macular Degeneration Treatment, *Iranian Journal of Chemistry and Chemical Engineering (IJCCE)*, **41(9):** 2900-2909 (2022).

[78] Abou El Fadl F.I., Maziad N., El-hamouly S., Hassan, H.E., Magnetically Responsive Nanocomposite Hydrogels for Controlled Release of Ciprofloxacin, *Iranian Journal of Chemistry and Chemical Engineering (IJCCE)*, **40(9)**: 2873-2885 (2021).

[79] Sheibani S., Zare K., Mousavi Safavi S.M., The Effects of pH and Chelating Agent on Synthesis and Characterization of Ni Mo/γ-Alumina Nanocatalyst for Heavy Oil Hydrodesulfurization, *Iranian Journal of Chemistry and Chemical Engineering (IJCCE)*, **40(1)**: 21-34 (2021).